Journal of Applied Electrochemistry **32**: 455–465, 2002.

Current–voltage behaviour of bipolar membranes in concentrated salt solutions investigated with chronopotentiometry

F.G. WILHELM, N.F.A. van der VEGT*, H. STRATHMANN and M. WESSLING
Membrane Technology Group, Faculty of Chemical Technology, University of Twente, PO Box 217, 7500AE Enschede, The Netherlands
*(*author for correspondence, fax: +31 53 489 4611; e-mail: N.F.A. vanderVegt@ct.utwente.nl)*

Received 5 October 2001; accepted in revised form 31 January 2002

Key words: bipolar membrane, chronopotentiometry, concentration influence, dynamic electrical potential

Abstract

Chronopotentiometry is used as a tool to obtain detailed information on the transport behaviour of the bipolar membrane BP-1 in solutions of high sodium chloride concentration above the limiting current density. We discuss critically the interpretation of the observed transition times. The occurrence of two such polarization times for low to moderate current densities is explained by the membrane asymmetry: the two membrane layers of opposite charge in general have different transport properties such as co-ion concentration and diffusion coefficient. The reversible and irreversible contributions to the transmembrane potential can be distinguished which allows the bipolar membrane energy requirements to be addressed. The experiments indicate that the increased voltage drop across bipolar membranes observed with higher solution concentrations can be explained on the basis of stronger concentration gradients in the membrane layers. The gradients become stronger with increased current density, but here the ohmic resistance under steady state transport conditions (the transport resistance) contributes to the increasing electrical potential. The transport resistance decreases with increasing current density due to the ion-exchange of the salt counter ions with the water splitting products. The experiments show that bipolar membranes should be operated at low current densities and low concentrations to minimize energy requirements. These findings are in contrast to the high current densities required to reduce impurities in the produced acid and base.

List of symbols

A	anion permeable layer of the bipolar membrane
C	cation permeable layer of the bipolar membrane
$c_{\mathrm{fix},\bar{c}}(c_{\mathrm{fix,a}})$	fixed charge density of the cation- (anion-) permeable layer (mol l^{-1})
c_i	molar concentration of species i (mol l^{-1})
$\bar{c}_{\mathrm{m},0}$	averaged ion concentration in the membrane (mol l^{-1})
D_i	apparent ionic diffusion coefficient (m^2 s^{-1})
D_{av}	average apparent diffusion coefficient of the electrolyte (m^2 s^{-1})
F	faradaic constant (96 485 A s mol^{-1})
j	current density (mA cm^{-2})
J_i	flux of ion i (positive in direction of positive current) (mol m^{-2} s^{-1})
r	area resistance (Ω cm^2)
s	membrane layer thickness (m)
t	time (s)
t_0	switch-on time (s)
t_1	switch-off time (s)
t_C	transition time (s)
t_D	discharging time (s)
t_i	(migrational) transport number of the ion i
t_P	polarization time (s)
U	electrical potential difference (V)
z_i	charge number of the ion i including sign

Subscripts and superscripts

co	co-ion
counter	counter ion
critical	at critical current density
equ	equilibrium state
ini	initial value
m	measured value
max	maximum value
mem	in or across the membrane
off	at current switch off
S	solution
stat	steady state transport
transp	transport state

1. Introduction

Bipolar membranes, laminates of cation and anion permeable membranes can split water into protons and hydroxide ions with the help of an electric field. These membranes are used in electrodialysis modules to produce acids and bases from neutral salts. Water splitting in bipolar membranes is a proton transfer reaction whereas at electrodes it involves reduction and oxidation reactions, often resulting in gas production. The relatively mild chemical environment makes bipolar membrane electrodialysis (ED-BPM) suitable for the production or separation of sensitive organic acids [1]. In the early stages of development of bipolar membrane technology, ED-BPM was seen as a competitive process to electrolysis and a promising method for the large scale production of concentrated sodium chloride and inorganic acids, such as hydrochloric acid or sulfuric acid. The main reason was the theoretically lower energy consumption with bipolar membranes because the energy consumed in producing gases as side products could be avoided. However, this energy margin shrunk with the developments in electrolysis, especially with the introduction of gas diffusion electrodes. Another reason why bipolar membrane electrodialysis is not used for the large scale production of inorganic acids and bases is salt ion leakage across the bipolar membrane especially at increased product concentrations resulting in undesired salt impurities in the acid and base product [2]. Salt ion leakage can be reduced by operating at low product concentrations or at high current densities.

Today, the major advantages of bipolar membrane electrodialysis are found in process integration, for instance in fine chemicals production [3] where some impurities are tolerable, for example, in streams that are fed back into unit operations before the bipolar membrane unit. If bipolar membrane electrodialysis can provide the acid and base at sufficient concentrations and purity, the main advantages lie in the lower amount of acid and base to be supplied, the reduction of salt waste streams, and the integrated product purification or conversion. Indeed, such promising processes need design guidelines how the bipolar membrane and the process should be designed for operation at optimised conditions, such as sufficient product purity and low energy utilization.

In this paper, the energy requirements of water splitting with a bipolar membrane exposed to different, relatively high, salt solution concentrations are investigated using chronopotentiometry. This is a dynamic electrochemical characterization technique that allows various contributions to the overall electrical potential difference under steady state transport conditions of the bipolar membrane to be distinguished by recording the dynamic response to a current step function [4]. This paper focuses on discussion of the observed transition times and the energy requirements to split water in a bipolar membrane, both related to the membrane transport processes. Of special interest is the question how much energy is lost by undesired transport processes and to obtain information as to how closely the theoretical energy requirements are approached. This is investigated by characterizing the behaviour of a bipolar membrane at increased solution concentrations. The bipolar membrane BP-1 from Tokuyama Corp., Japan, is used for these studies because it has been widely available and it is one of the farthest developed membranes with respect to energy requirements, selectivity and stability.

2. Theory

2.1. *BPM chronopotentiometry: principle and characteristic values*

Before chronopotentiometric measurements the membrane should be equilibrated in a salt solution. In one chronopotentiometric sequence, the electrical potential drop across the bipolar membrane is recorded with time after setting the current or the current density to a fixed value at time t_0 and switching it off at time t_1. When switching on the current, the potential drop across the membrane is changing until a steady-state value is reached. When the current is switched off, this potential drop relaxes back to zero.

Two current density regions are distinguished when the bipolar membrane is operated in a salt solution of neutral pH. At sublimiting currents, only salt ions are transported and the salt ion concentration in the bipolar membrane junction has a finite value, much higher than the concentration of protons and hydroxide ions in the interface which lies in the same range as found in free water (10^{-7} mol l^{-1}). When the limiting current density j_{LIM} is applied, the overall electrical resistance of the bipolar membrane reaches a maximum. Due to internal concentration polarisation, the co-ion concentration in the membrane at the junction of the two ion conductive layers approaches zero while no extra protons and hydroxide ions are available yet for conduction of the current [2]. In the over-limiting region, water splitting occurs in the junction of the two ion conductive layers of the bipolar membrane. Switching on such a current, first the salt co-ions are removed from the bipolar membrane junction and, as soon as water splitting starts, additionally the counter-ions in the membrane layers are partially exchanged with the water splitting products [4].

A typical chronopotentiometric curve obtained in the over-limiting region (see Figure 1) shows certain characteristic values. The initial switch-on jump of the electrical potential difference across the membrane at t_0 and the immediate breakdown after switching off the current at t_1 are due to the ohmic resistances of the membrane layers in equilibrium with the surrounding solution and the ohmic resistance in the transport state, respectively. In the beginning the concentration profiles of the salt ions in the two layers of the bipolar membrane are horizontal (outside the electrical double

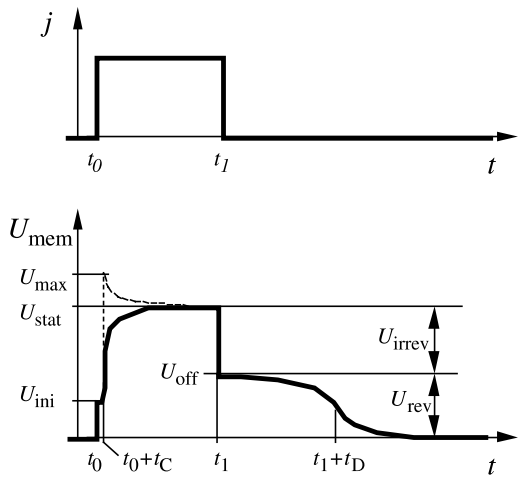

Fig. 1. Schematic potential response of a bipolar membrane with a constant current in the over-limiting range switched on at time t_0 and off at time t_1. Overshoot potential $U_{m,max}$ is observed at high current densities only.

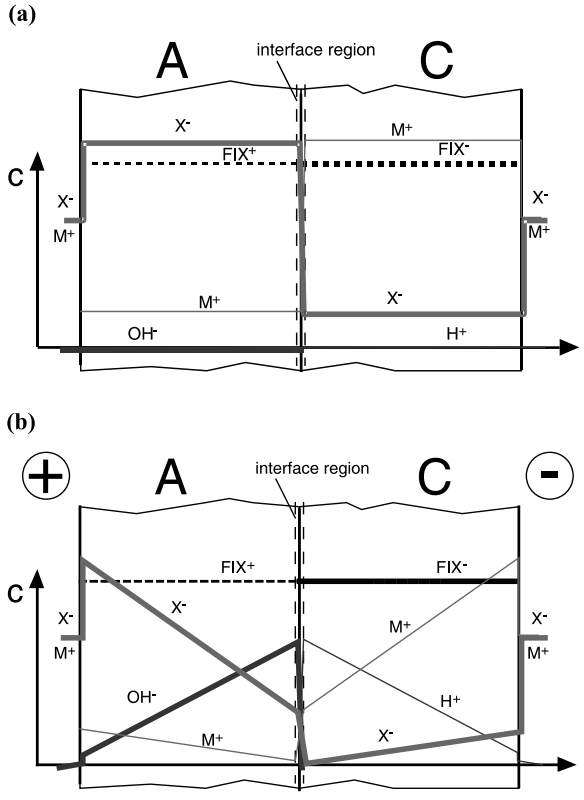

Fig. 2. Schematic concentration profiles in the anion and cation permeable layers of a bipolar membrane (a) in equilibrium at switch-on and (b) under steady state transport conditions at switch-off.

layers), Figure 2(a). In contrast, the concentration profiles show strong gradients under steady state transport conditions which result from salt co-ion depletion and production of hydroxide ions and protons in significant amounts by the water-splitting reaction in the bipolar junction, Figure 2(b). The salt ion depletion of the membrane layers increases the electric resistance whereas the water splitting products can reduce it due to the relatively high ionic mobility. The transition time t_C, as outlined in more detail below, is the intermediate time after switching on the current at which the ion exchange material next to the bipolar junction is virtually completely depleted of co-ions.

The electrical potential U_{off} remaining after switching off the current is also called the reversible potential, in contrast to the irreversible potential (U_{stat}–U_{off}) which represents the energy loss due to the ohmic resistance of the bipolar membrane in the transport state [4]. The reversible potential is a result of the strong concentration gradients of the mobile ions and, for its main part, the recombination reaction of protons and hydroxide ions in the bipolar junction. The transport processes occurring after the current switch-off allow the recombination reaction to proceed until it terminates due to the lack of reactants. The discharging time τ_D at which the steepest drop in the dynamic electrical potential is observed after switching off the current, is related to this termination of the recombination reaction.

2.2. *Transition times*

The transition time is one of the characteristics we can read from the chronopotentiometric response curve of a bipolar membrane when an overlimiting current density is applied. Its relation with the membrane layer transport properties is complex for such a two-layer system whereas the considerations about the reversible and irreversible energy usage of bipolar membranes are rather straightforward. In the chronopotentiometric response curve, the transition time is the time with the steepest increase of the electrical potential. First, the interface region is depleted of co-ions and the potential increases steadily until water splitting products become available when the electrical potential difference across the bipolar junction is large enough. As a result of this, the electrical conductivity is reduced and then increases again. In fact, at high current densities the water splitting can be strong enough to cause a reduction of the electrical potential so that the curve with the current imposed shows a distinct maximum as indicated in Figure 1.

Analytical solutions to calculate the transition times have been presented for some special cases: (i) the dynamic transport equations in the homogeneous diffusion boundary layer at electrodes or cation and anion permeable membranes, and (ii) the internal concentration polarization in a quasi-symmetric bipolar membrane having two layers only differing in sign of the fixed charges have been solved with the help of Laplace transformations [5–8]. The transition time t_C for the depletion of the bipolar membrane layers has been determined with quite similar assumptions as for the diffusion layer of the solution in case (i), such as homogeneous and constant layer properties and semi-infinite layer thickness as discussed below [8]:

$$t_C = \pi D_{av,m}\left(\frac{\bar{c}_{m,0}F}{2j\left(t_{i,C} - t_{i,A}\right)}\right)^2 \quad (1)$$

Here, $D_{av,m}$ is the average diffusion coefficient in the membrane layer and j is the current density. The transport numbers $t_{i,C}$ and $t_{i,A}$ of the ionic species i (salt anion X or salt cation M) in the cation and anion permeable layer, respectively, are assumed to be symmetric to the interface according to $t_{i,C} = 1 - t_{i,A}$ and, with the closing condition, for example, $t_{X,C} = t_{M,A}$. The concentration $\bar{c}_{m,0} = \left(c_{co,0}c_{counter,0}\right)^{0.5}$ is the initial virtual salt concentration at time t_0 in the bipolar membrane layers [8]. At the transition time this concentration reaches zero in the bipolar junction and, according to theory, the co-ion concentration also reaches zero (but with a different exponent as seen in the defining equation for the virtual salt concentration). This equation yields a linear relationship between the transition time against the inverse current density squared (also known as a Sand plot) when all the assumptions hold [5, 8]. The average diffusion coefficient used in this equation is obtained from:

$$D_{av} = \frac{2D_{co}D_{counter}}{D_{co} + D_{counter}} \quad (2)$$

Equation 1 has been derived with the questionable assumption of constant migrational transport numbers that correspond to the state of the membrane in equilibrium with the surrounding salt solution. The migrational transport number t_i of any ionic species (traditionally just called the transport number [9]) can be estimated from ion concentrations and the apparent ion diffusion coefficients in solutions of a 1:1 electrolyte from the Nernst–Planck equations [9]. When concentration gradients are absent it reads:

$$t_i = \frac{c_i D_i}{\sum_k c_k D_k} \quad (3)$$

This indicates that the migrational transport number depends on the diffusion coefficients but also on the ratios of the ion concentrations. In ion permeable membranes the latter effect is dominant. With an increasing concentration of electrolyte in the surrounding solution, both the co-ion and the counter-ion concentrations in the membrane increase by the same absolute amount; however, the ratio of co- to counter-ion concentration in the membrane changes, it approaches unity. Hence the migrational transport number is not a membrane constant. The same holds for the generalised or actual transport number which is calculated from the fluxes at the actual transport conditions, including ionic concentration gradients [10].

Thus, it is obvious that determining transport numbers (and hence, a measure of the membrane selectivity) from measured transition times t_C can not be straightforward. In spite of the critical notes, transition times are well suited as qualitative measures of bipolar membrane selectivities as we will show below. Therefore, we compare the observed transition times with selectivity criteria obtained from the limiting current density of a current voltage curve. A high limiting current density indicates a high salt ion flux [2].

Another critical issue is the thickness of the diffusion layer. The derivation of the transition time is based on the assumption of infinitely thick diffusion layers, the semiinfinite boundary layer [6, 8, 11]. In contrast, the diffusion layers encountered in electrochemical systems in general have a finite thickness. For a bipolar membrane, not only the depletion process at the bipolar junction but also the salt fluxes across the membrane–solution interfaces cause changes in the concentration profiles in the membrane layers. To have a negligible influence of such a second boundary, the effective thickness of the diffusion layer at time t must be smaller than the thickness of the actual membrane layer. The semi-infinite layer assumption holds if the root of the mean square displacement at the transition time, $\langle x^2\rangle^{1/2}$ is smaller than the layer thickness s [6]:

$$s > \langle x^2\rangle^{1/2} \equiv \left(2D_{av,m}t_C\right)^{1/2} \quad (5)$$

To use this equation, we eliminate the transition time with Equation 1. Then a critical current density can be calculated, above which a bipolar membrane layer can be regarded as semiinfinite:

$$j > \left(\frac{\pi}{2}\right)^{1/2} D_{av,m}\frac{\bar{c}_{m,0}F}{s\left(t_{i,C} - t_{i,A}\right)} \equiv j_{critical} \quad (6)$$

When the two layers of a bipolar membrane show different transport properties two different critical current densities can be calculated. It becomes clear that the derivation of Equation 1 includes many simplifying assumptions. However, this equation is useful when studying trends and to explain phenomena observed in the membrane transport behaviour. In this paper, we use it to investigate bipolar membranes at increased electrolyte concentrations where the transport processes are even less ideal.

3. Experimental details

The six compartment membrane module used for the experiments is described in more detail in [4]. It utilises a four electrode arrangement with working electrodes of stainless steel (cathode) and platinum coated titanium (anode). Calomel electrodes with salt bridges (Haber–Luggin capillaries) are used as reference electrodes. The temperature of the solutions next to the membrane under investigation is controlled at 25 °C within 0.2 °C with a laboratory thermostat and two glass-coil heat exchangers. The power supply is controlled by a

Table 1. Characteristic values of the bipolar membrane BP-1 in sodium chloride solutions according to [12, 13]

	d_{layer} /mm	$10^{12}\ D_{Na^+}$ /m^2 s^{-1}	$10^{12}\ D_{Cl^-}$ /m^2 s^{-1}	c_{FIX} /mol l^{-1}	c_S /mol l^{-1}	c_{Na^+} /mol l^{-1}	c_{Cl^-} /mol l^{-1}	t_{CO} /-(*)
Anion	0.06	40	70	1.5	1.0	0.07	1.57	0.026
Permeable					2.0	0.19	1.69	0.059
Layer					4.0	0.44	1.94	0.114
Cation	0.15	90	60	1.5	1.0	1.563	0.06	0.023
Permeable					2.0	1.63	0.13	0.052
Layer					4.0	1.85	0.35	0.111

*Calculated with Equation 3.

computer through an analogue interface to follow the desired measurement program. Both, the current through the cell and the voltage across the reference electrodes are measured through separate isolation amplifiers and recorded with the computer in time with a rate of 10 samples per second. At very high current densities, the switch-off characteristics of the power supply (power source without load functionality) do not allow for an accurate reading. The response of the power supply, a Delta Electronica ES 030-5 for the current to reach zero at switch-off is slow for current densities of about 30 mA cm^{-2} and above. At switch-off below this current density and for all current densities at switch-on, the characteristics of the power supply are well suited for these experiments.

Series of chronopotentiometric measurements are recorded by imposing the desired current density for the desired time-span of about 20 min, then switching off this current by setting the cell voltage to 0 V for another twenty minutes to allow the membrane to reach equilibrium with the surrounding solution. After such a period of the current imposed and then switched off, the next current is applied with an increased current density. The length of the time interval with zero cell voltage has been chosen long enough to reach equilibrium, that is, until the potential drop across the membrane reaches zero.

A second set of experiments is performed to investigate the influence of the current-on time on the switch-off characteristics. This is done by imposing the same current density in consecutive switch-on periods for a different time-span in an irregular series of 120 s, 600 s, 60 s, 300 s, 31 s before switching off. Because the present reactants determine the discharging time, it should not change if a steady transport state has been reached. In contrast, if the current is switched off before the steady state is reached, the discharging time t_D should decrease with shorter switch-on times as a consequence of the reduced extent of ion exchange in the membrane. However, an increasing t_D in consecutive experiments in this irregular series indicates changes in solution properties (e.g., a pH shift) or a poor reequilibration between consecutive experiments. Thus, we can distinguish if a change in discharging time from one experiment to the other is due to changes of the solution concentration from one experiment to the next or due to a different transport state of the membrane itself. We studied the effect of different switch-on time-spans for current densities of 1.4, 4.3, 33 and 102 mA cm^{-2} for a solution containing 1.0 mol l^{-1} sodium chloride.

The membrane investigated is the bipolar membrane BP-1 from Tokuyama Corporation, Japan. The properties of the anion exchange membrane AMX and the cation exchange membrane CMX (both Tokuyama Corp.) [12] are used as the transport parameters for the layers of the membrane BP-1 (Table 1). With the exception of the membrane thickness, we assume the properties of the separate layers of BP-1 to be equal to the ones of the monopolar membranes since they are prepared of very similar materials [12, 14].

4. Results and discussion

4.1. *Steady state current–voltage curves*

Steady state current–voltage curves of the membrane BP-1 at different solution concentrations are shown in Figure 3(a). They are recorded by the current-sweep method; how closely they approach the steady state is discussed in [4]. The measured electrical potential has been corrected for the solution resistance to obtain the electrical potential difference over the membrane. (The measured area solution resistance is 9.084, 5.148 and 3.367 Ω cm^2 for the sodium chloride concentrations of 1.0, 2.0 and 4.0 mol l^{-1}, respectively.) These steady state current–voltage curves show the typical behaviour with three distinct areas, easily distinguished in Figure 3(b): (i) At low current densities the current is conducted by the salt ions, (ii) the limiting current density plateau corresponds to internal concentration polarization, and (iii) in the overlimiting region the desired water splitting occurs in parallel to the undesired salt ion transport.

As discussed above, at the limiting current density the electrical charge is transported across the bipolar membrane entirely by the salt ions. The limiting current density should depend on the solution concentration in a quadratic manner assuming constant and symmetric membrane properties and omitting ion activity coefficients in the considerations [2]. The measured limiting current densities (see Table 2) do not follow such a

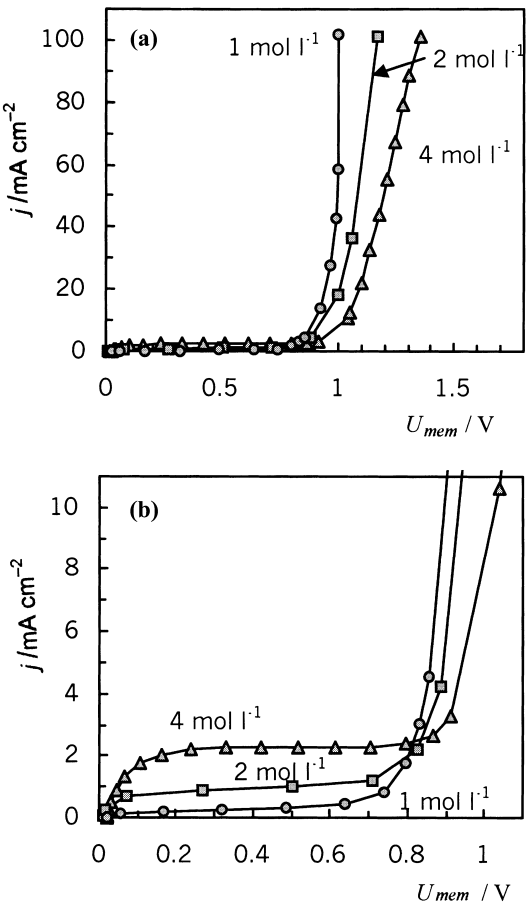

Fig. 3. Steady state current voltage curves of bipolar membrane BP-1 in different concentrations from current–voltage sweeps (points above 100 mA cm^{-2} are the final values of the chronopotentiometric response curves with the respective current density). (a) Entire curve; (b) detail at low current densities.

Table 2. Polarization behaviour of the membrane BP-1 at a current density of about 100 mA cm^{-2} in concentrated sodium chloride solutions

c_S/mol l^{-1}	1.0	2.0	4.0
j_{LIM}/mA cm^{-2}	0.33	1.0	2.3
j_{actual}/mA cm^{-2}	102	102	101
$r_{equil,av}$/Ω cm^2	10.2	8.5	7.1
$U_{mem,ini}$/V*	1.04	0.87	0.72
$U_{mem,max}$/V	1.54	1.64	1.83
$U_{mem,max} - U_{mem,ini}$/V	0.50	0.77	1.11

*Calculated with the average membrane resistance $r_{equil,av}$ and the actual current density j_{actual}.

quadratic relation, that can indicate that the limiting current in the high solution concentrations is over-predicted with the simplified model where it should follow a quadratic relation. This discrepancy stems from the overestimation of the co-ion concentration with the Donnan equilibrium. Membranes are non-homogeneous and have high local concentrations of ion exchange groups, resulting in a better co-ion exclusion than what is expected from the overall fixed charge density c_{FIX} in the homogeneous model. Furthermore, many of the membrane properties (diffusion coefficient, fixed charge density etc.) change at increased solution concentrations due to lower water contents in the membrane layers.

The steady state electrical potential for currents above the limiting current density is clearly higher for the higher concentrations (Figure 3(a) and (b)). This has also been found with an appropriate theoretical model in [12]. With chronopotentiometry, we can separate the contributions to the steady state electrical potential and relate them to specific concentration profiles and transport conditions in the membrane layers.

4.2. *Chronopotentiometric response curves*

All the curves in Figure 4(a)–(c) are chronopotentiometric responses with currents above the limiting current density for the respective sodium chloride concentration in the solution. The measured electrical potential U_m displayed in these graphs is not yet corrected for the solution resistance (see above) to yield the electrical potential of the membrane, U_{mem}. The characteristics of some curves can only be distinguished in the numerical data, however, all show the typical shape (Figure 1) with an initial jump, then a slowly increasing electrical potential, up to the transition time with a maximum slope.

Above a current density of 11 mA cm^{-2}, all the curves show an overshoot in the electrical potential after the transition time t_C. As discussed in [4], the overshoot is an indication of the sequential processes occurring in a bipolar membrane: first the concentration profiles of co-ions develop, then water splitting starts and the salt counter-ions are partially exchanged against water splitting products. The shape of the overshoot is similar for the curves with about the same current density independent of the solution concentration. The maximum voltage across the membrane at about 100 mA cm^{-2}, presented in Table 2 is higher for the higher solution concentration. The polarization voltage, that is, the difference between the maximum and the initial voltage shows an even stronger concentration dependence; thus, the polarization becomes stronger for higher solution concentrations.

After the transition time or the overshoot, the electrical potential reaches a stable value except for the four molar solution with the current densities 2.4 and 3.2 mA cm^{-2} (Figure 4(c)). For the other curves, the time to reach the steady state can be determined from the chronopotentiometric curves. This time is different for the different regions in the current–voltage curve. With the high solution concentrations used in these investigations, the steady state electrical potential in the vicinity of the limiting current density is not reached after five minutes. The time to reach steady state increases with increasing solution concentration because the number of ions to be transported out of the membrane layers is higher. For the curve with 2.4 mA cm^{-2} significant co-ion depletion next to the bipolar junction does not occur within 20 min.

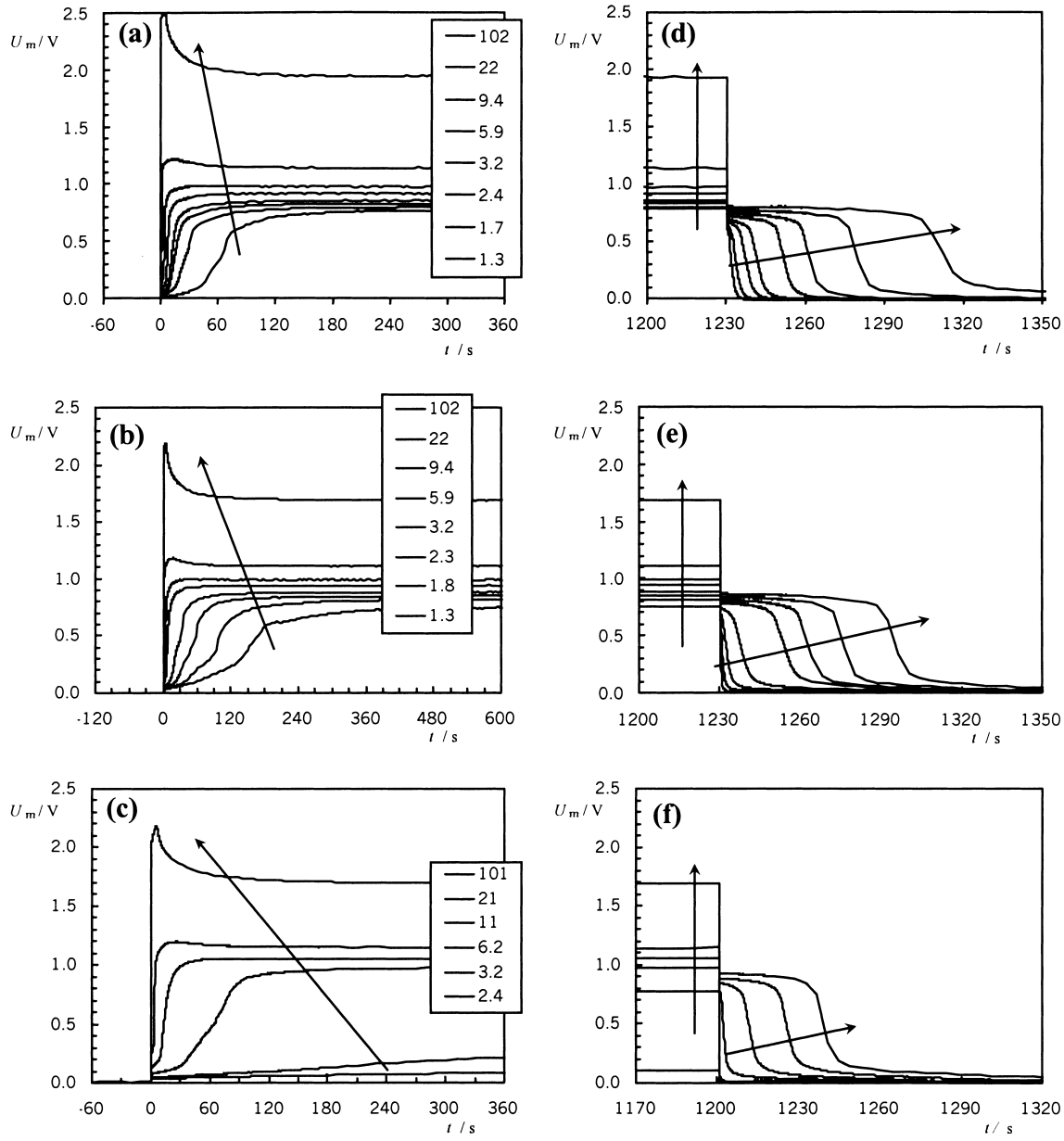

Fig. 4. Chronopotentiometric response curves of the membrane BP-1 (sodium chloride, 25 °C) at different applied current densities j/mA cm^{-2} as indicated, not corrected for the solution resistance. Legend order corresponds to the order of the curves; arrows indicate an increasing current density. Switch-on: (a) 1, (b) 2, (c) 4, and switch-off, (d) 1, (e) 2 and (f) 4 mol l^{-1}.

4.3. *Transition time*

The transition times determined from the numerical data for all the runs are presented in Figure 5 in a Sand-type plot. In general, as expected, the longer transition times are observed for higher solution concentrations and lower current densities. Approximately linear relationships are obtained for the sodium chloride concentrations of 1.0 and 2.0 mol l^{-1} with high current densities. However, most of these transition times are obtained for current densities where the semiinfinite layer assumption obviously is violated (Equation 6, see Table 3). Nonetheless, the linear relationship indicates that the influence of the interface with the solution does not influence the ion transport in the membrane significantly. The nonlinear behaviour in Figure 5 at the high concentration of 4.0 mol l^{-1} and with the other concentrations at very low current densities indicates that the changes of transport properties in the membrane layers (e.g., the apparent diffusion coefficient or the activity coefficients) in time are no longer negligible.

In Table 3 we compare the transition time for current densities where the semi-infinite layer thickness assumption is valid. The slope $t_C j^2$ of the Sand-plot is reported. The data points taken from Figure 5 to estimate the slope of the measured data, the 'measured $t_C j^2$', include only the ones above the calculated critical current density (including the origin). This slope is listed next to the slope calculated according to Equation 1 on the basis of the given membrane properties, the 'calculated

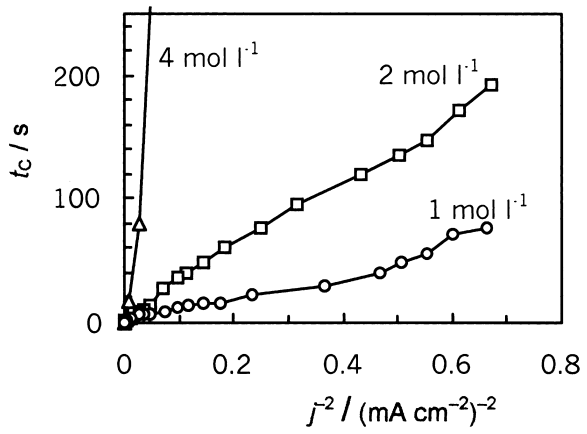

Fig. 5. Transition time of the membrane BP-1 for different solution concentrations depending on the current density in a plot according to Sand.

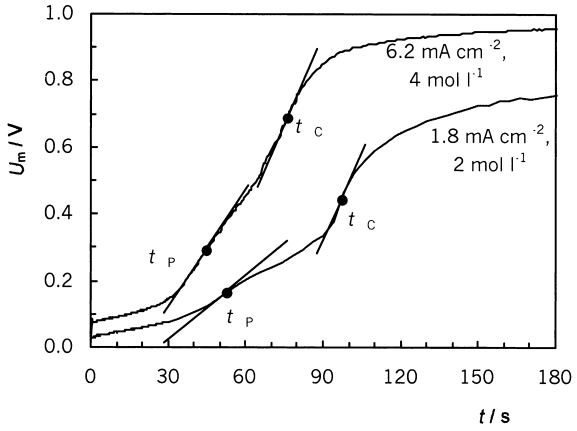

Fig. 6. Chronopotentiometric response curves with two transition times of the bipolar membrane BP-1 in sodium chloride solutions at 25 °C.

$t_C j^2$'. For both, the measurements and the calculations, the slope is larger with an increased solution concentration. A larger slopes indicates a longer transition time for the same current density and, as discussed above, a lower membrane selectivity. This is in agreement with the lower selectivities for higher concentrations indicated by the increased limiting current densities in Table 2.

For the two layers, different critical current densities are calculated due to the different layer properties. Therefore, we use different sets of measurement points to estimate $t_C j^2$ and it is different for the two membrane layers at the same concentration. In contrast, the calculated slopes differ for the two layers because the ion concentrations and the diffusion coefficients differ in both layers (the membrane is asymmetric). The calculated dependence of the transition time on the concentration represents the measured data well, considering the measurement accuracy and despite the assumptions made for the calculation.

Some of the chronopotentiometric response curves show an interesting phenomenon in the switch-on period of the electrical current: After the initial jump, they show a double-S shape; in Figure 6 this becomes more obvious by zooming in. The slope of the first inflection point at time t_P is lower than the slope of the second inflection point, the actual transition time t_C. For example, for the 4 mol l^{-1} solution with a current density of 6.2 mA cm^{-2}, the two corresponding times are $t_P = 45$ s and $t_C = 77$ s or for the 2 mol l^{-1} solution with a current density of 1.8 mA cm^{-2}, the two corresponding times are $t_P = 51$ s and $t_C = 96$ s. In the chronopotentiometric response curves in Figure 4(a)–(c), such a double-S shape is also observed with other concentrations and current densities, that is, this phenomenon is reproducibly recorded. In the numerical data, the two times can be distinguished with current densities between approximately 2 and 10 times the limiting current density. Below two times the limiting current density, the curves do not show a steady increase but some low-frequency noise; above about ten times the limiting current density, the resolution of the measurement in time is not high enough.

These two characteristic times can be considered as the different polarization times of the depletion regions in the two membrane layers next to the bipolar junction. The membrane-solution interfaces are not involved because they do not show depletion behaviour at such low current densities and high salt concentrations. The two polarization times are a result of the bipolar membrane asymmetry. In the first layer, the co-ion

Table 3. Comparison of calculated and measured relation of transition times with current density

c_S /mol l^{-1}	Layer	d /mm	$j_{critical}$ /mA cm^{-2}(∗)	Points at or above $j_{critical}$	Measured $t_C j^2$ /mA^2 s cm^{-4} (†)	Calculated $t_C j^2$ /mA^2 s cm^{-4} (‡)	$\frac{(t_{Cj^2})_A}{(t_{Cj^2})_C}$
1.0	A	0.06	37	2	530	490	0.96
	C	0.15	18	5	470	510	
2.0	A	0.06	66	1	2900	1500	1.07
	C	0.15	31	3	940	1400	
4.0	A	0.06	122	0	–	5300	0.95
	C	0.15	60	1	4500	5600	

*Calculated with Equation 6 using the data in Table 1 for the respective membrane layer.
†Obtained by a linear fit of measurements for currents above the critical current density for the respective layer through the origin.
‡Calculated with Equation 1 using the diffusion coefficients and co-ion concentrations in Table 1.

concentration reaches approximately zero at the polarization time t_P and the resistance increases significantly. However, the co-ions in the second layer are still available to transport the current and, thus, the resistance increase is limited. Water splitting starts only when the second layer is depleted as well and the electrical potential difference across the junction becomes large enough. The ratio of the calculated transition times of both layers (Table 3) is almost unity (within the experimental error), thus, it is much smaller than the ratio of the observed two polarisation times. The model with averaged diffusion coefficients and the virtual salt ion concentration in the membrane fails to predict these two times (i.e., it does not account for differences of co- and counter-ion transport). If we suppose mainly the co-ion transport to be responsible for the polarization behaviour and considering the coupling with the counter ions only by the averaged diffusion coefficient, the average concentration $\bar{c}_m^2$ in Equation 1 should be replaced by c_{co}^2. The squared ratio of the measured co-ion concentrations in the cation permeable layer over the one in the anion permeable layer (see Table 1) is 0.63 for 4 mol l^{-1} solutions and 0.47 for 2 mol l^{-1} solutions. These are approximately the ratios of the characteristic times in Figure 6. Thus, we take this as evidence that the hypothesis of asymmetric co-ion depletion is plausible. Based on the lower co-ion content of the cation permeable layer (Table 1) we thus conclude that this layer is depleted of co-ions first. Water splitting starts as soon as the anion permeable layer is fully depleted as well.

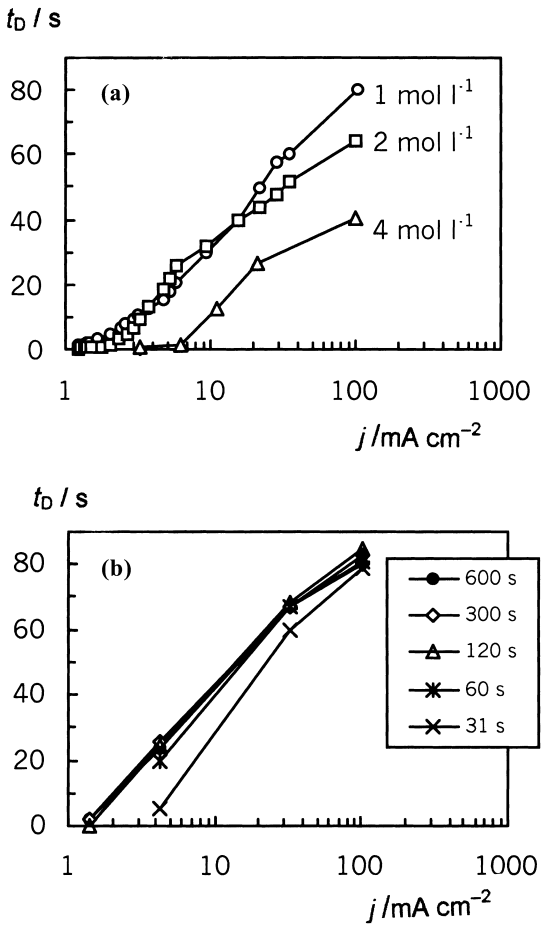

Fig. 7. Discharging times of the bipolar membrane BP-1 (a) for different solution concentrations after the current was applied for 20 min, and (b) for the current applied for different times with a solution concentration of 1 mol l^{-1}.

4.4. *Discharging time*

The times for discharge t_D depend on the solution concentration and current density as shown in Figure 7(a). The discharge times have been determined by analysis of the numerical data and were identified with the extrema in the slopes in Figure 4(d)–(f). The discharging time is longer for low concentrations and high current densities. As discussed in [4], two main transport processes are responsible for the relaxation of the concentration profiles in the bipolar membrane layers: (i) counter ions are exchanged across the membrane–solution interface; for example, in the anion exchange membrane, hydroxide ions are replaced by chloride ions; (ii) in the bipolar junction, the hydroxide ions in the anion exchange layer can recombine to water with the protons from the cation exchange layer because co-ions cross the bipolar junction. Only with this co-ion flux discharging is possible at zero-current conditions. Both processes are faster with an increased salt concentration in the solution.

The discharging times in Figure 7(b) are determined from curves with the current applied for different times. For curves where the steady state has been reached, the discharging time does not change anymore with an increasing current-on time. This can be used as a sharp criterion to decide if steady state conditions have been reached. As a criterion it is more precise than inspecting the chronopotentiometric switch-on curves for the steady transport state. The results in Figure 7(b) indicate that the steady state is reached faster for high current densities.

4.5. *Ohmic resistances*

The equilibrium resistance determined from the initial jump in the chronopotentiometric response curves is 10.2, 8.5 and 7.1 Ω cm^2 for the 1.0, 2.0 and 4.0 mol l^{-1} solution concentrations, respectively. It is lower with higher solution concentrations because the total ion content in the membrane is higher. A reduced water content in the membrane as expected with increased solution concentration apparently is not enough to counterbalance this effect.

The resistance of the membrane in the transport state is calculated with the irreversible potential drop when the current is switched off (Figure 1) according to $r_{transp} = (U_{mem,stat} - U_{mem,off})/j$ as derived in [4]. The ratio of this transport-state resistance over the equilibrium resistance is presented in Figure 8. The transport resistance is reduced with increasing current density due

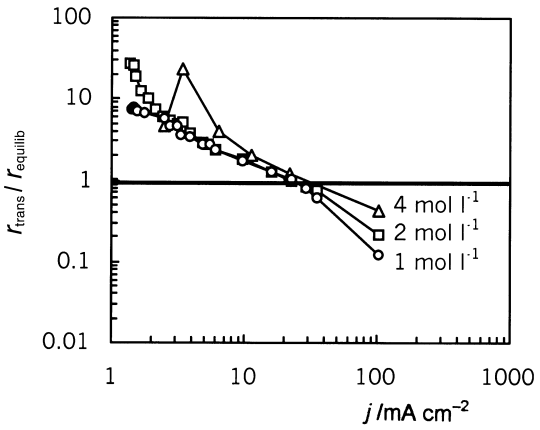

Fig. 8. Ratio of transport resistance over equilibrium resistance of BP-1 in sodium chloride solutions at 25 °C. Note: Steady state was not reached for 4 mol l^{-1} with 2.4 and 3.2 mA cm^{-2}.

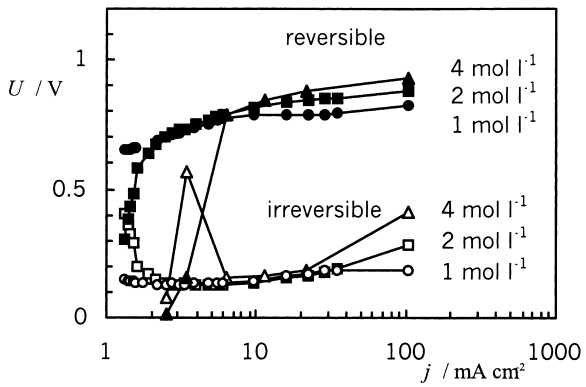

Fig. 9. Contributions to the transport-state electrical potential of the membrane, $U_{mem,stat}$ for different concentrations in the overlimiting current range. Note: Steady state was not reached for 4 mol l^{-1} with 2.4 and 3.2 mA cm^{-2}.

to the ion exchange of salt counter ions with water splitting products. The ratio of transport over equilibrium resistance drops below unity for current densities above 20 mA cm^{-2} for all three concentrations. As discussed in [4], at this current density the increase of the resistance due to salt ion depletion is balanced by the reduction of the resistance due to the ion exchange with water splitting products. For all three concentrations, this coincides with the current density where the overshoot is observed first in the chronopotentiometric response curves. It is not yet clear if these current densities coincide for every bipolar membrane. However, both phenomena are a result of the same processes in the membrane: co-ion depletion and ion exchange (i.e., salt counter-ion substitution by protons and hydroxyl ions in the respective layers).

The ratio of resistance in the transport state compared to the equilibrium state is higher for higher solution concentrations. To reach full co-ion depletion of the membrane layers at the bipolar junction with increased solution concentrations, more salt ions have to be removed, thus, the resistance increases more due to this stronger depletion.

4.6. *Reversible and irreversible potential*

The reversible and irreversible contributions to the steady state electrical potential in the over-limiting current density region are presented in Figure 9. The irreversible potential of the membrane, $U_{mem,irreversible} = (U_{mem,stat} - U_{mem,off})$ is the one actually used for calculating the transport resistance discussed above.

For the 4.0 mol l^{-1} solution, the internal concentration polarization is not yet significant after 20 min with a current density of 2.4 mA cm^{-2} (the overall electrical potential does not increase significantly within 20 min, Figure 4(c) and (f)), even though this current density is above the limiting current density. Both, the reversible and the irreversible contributions to the electrical potential difference are very small (Figure 9, triangles at the lowest current density). The irreversible contribution is already slightly higher than in equilibrium (Figure 8) but no water is dissociated and the reversible contribution is not significant. For the same solution with a current density of 3.2 mA cm^{-2}, the polarization is much stronger. At this current, the reversible contribution in Figure 9 indicates the presence of water splitting products. The irreversible contribution is very high due to the strong co-ion depletion. For higher current densities, this irreversible contribution is reduced because the water splitting products reduce the layer resistance as discussed above.

The curve with the 2.0 mol l^{-1} solution concentration shows a similar behaviour (open squares in Figure 9). Just above the limiting current density of 1.0 mA cm^{-2}, the irreversible potential is rather high, reaching a minimum at moderate current density and increasing again with further increasing currents. The reduction in transport resistance with increasing current (by the increased concentration of water splitting products) is enough to reduce the irreversible potential or to keep it stable for moderate current densities up to about 10 mA cm^{-2}; however, at high current densities the irreversible electrical potential difference increases – the reduction of the resistance (Figure 8) is of a smaller order than the increase of the current density. The phenomenon of ion exchange of the salt counter-ions occurs because the membrane is immersed in a neutral salt solution. In electrodialysis with the acid next to the cation exchange side of the bipolar membrane and the base next to the anion exchange side, such an ion exchange will not occur. The transport resistance will more likely be constant and the irreversible potential is expected to increase linearly with the current density.

At high current densities of comparable values, the irreversible contribution increases with the salt ion concentration. This is in contrast to the equilibrium resistance which is lower for increased concentrations. We attribute this to the amount of salt ions that are transported across the bipolar membrane: The flux of

salt ions is higher with increased concentration as indicated by the limiting current density, thus, fewer water splitting products are produced and available for ion transport. With the lower diffusion coefficients of the salt ions compared to the water splitting products, the overall resistance is higher and a higher electrical potential is necessary to conduct the imposed current.

The reversible potential slightly increases with increasing current density. This is interpreted as a result of the increasing content of water splitting products as the respective counter-ions in the membrane layers. For 1 and 2 mol l^{-1} solutions, the reversible potential appears to level off. This is due to the limited ion exchange capacity of the membrane layers. It happens earlier for the lowest solution concentration, whereas the current density for the full ion exchange has not been reached for the 4.0 mol l^{-1} solution (Figure 9, full triangles). Further, the reversible contribution is higher for the higher solution concentration, also in the areas where the potential has levelled off. We can attribute that to the higher contribution of the concentration gradients of co- and counter-ions in the membrane layers according to the electrochemical potential. The counter-ions are mainly the water splitting products with a high ionic diffusion coefficient compared to the salt ions.

5. Conclusions and recommendations

With chronopotentiometry it is possible to obtain insights in the transport behaviour of bipolar membranes at increased solution concentrations. The transition time, indicating the start of the water splitting in the chronopotentiometric response curves, is useful for indicative purposes. However, the two depletion regions on the two sides of the bipolar junction with different transport properties do not allow a quantitative analysis with the current theory. The transport processes are more complex as indicated by the observed second polarization time.

This experimental study allows an explanation of the increased electrical potential differences across the bipolar membrane with increased current density or increased solution concentrations. It is mainly due to the transport processes in the membrane layers and not directly in the membrane junction. In the membrane layers, the concentration profiles become stronger developed for higher concentrations and for higher currents. Only at very high currents, the salt counter ions next to the bipolar junction are completely exchanged with the water splitting products.

The concentration profiles influence both, the reversible and the irreversible contribution to the transport-state electrical potential difference. The increase of the reversible contribution is attributed to the increased electrochemical potential with increased concentrations and concentration gradients. The increase of the irreversible energy becomes higher with higher current densities or higher solution concentrations due to the energy losses at the ohmic resistances of the membrane. The reduction of the transport resistance observed with increased current density – not enough to reduce the irreversible potential – is not to be expected during acid–base production because then the discussed ion exchange of counter-ions does not occur.

Thus, from an energy point of view, bipolar membranes should be operated at low current densities. This is in contrast to the recommendations in [2] to obtain high membrane selectivity by increasing the current density. The irreversible energy losses can be reduced by operating bipolar membranes at low solution concentrations. This is in line with the recommendations for reduced salt ion transport. For the design of a bipolar membrane electrodialysis process, these two recommendations have to be balanced with the desire to operate with the highest possible current density and solution concentrations for low investment costs due to less required membrane area.

References

1. G. Pourcelly, *in* A.J.B. Kemperman (Ed.), 'Handbook on Bipolar Membrane Technology', (Twente University Press, Enschede, Netherlands, 2000), chapter 2.
2. F.G. Wilhelm, I. Pünt, N.F.A. van der Vegt, M. Wessling and H. Strathmann, *J. Membr. Sci.* **182** (2001) 13.
3. V. Cauwenberg, J. Peels, S. Resbeut and G. Pourcelly, 'Application of Electrodialysis within Fine Chemistry,' Book of Abstracts, Vol. 1, Euromembrane 1999, 19–22 Sept., Leuven, Belgium (1999), p. 109.
4. F.G. Wilhelm, N.F.A. van der Vegt, M. Wessling and H. Strathmann, *J. Electroanal. Chem.* **502** (2001) 152.
5. H-W. Rösler, F. Maletzki and E. Staude, *J. Membr. Sci.* **72** (1992) 171.
6. H-W. Rösler, PhD thesis, Universität GH Essen, Germany (1991).
7. J.J. Krol, M. Wessling and H. Strathmann, *J. Membr. Sci.* **162** (1999) 155.
8. N.P. Gnusin, V.I. Zabolotskii, N.V. Shel'deshov and N.D. Krikunova, English trans. *Elektrokhimiya* **16** (1980) 49.
9. J.O'M. Bockris, A.K.N. Reddy, 'Modern Electrochemistry 1 – Ionics', 2nd edn (Kluwer Academic/Plenum Publishers, New York 1998).
10. F.G. Wilhelm, PhD thesis, Universiteit Twente, Enschede (2001).
11. N.V. Shel'deshov, N.P. Gnusin, V.I. Zabolotskii, N.D. Pis'menskaya, English trans. *Elektrokhimiya*, **21** (1985) 152.
12 W. Neubrand PhD thesis, Univeristät Stuttgart, Germany (1999) (also published by Logos, Berlin, 1999).
13. W. Neubrand and G. Eigenberger, 'Equilibrium and transport properties of CMX and AMX membranes in aqueous solutions of NaCl and HCl' Poster printout and Book of Abstracts, Euromembrane, June 1997, University of Twente, Enschede, The Netherlands (1997).
14. F.G. Wilhelm, N.F.A. van der Vegt, M. Wessling and H. Strathmann, *in* A.J.B. Kemperman (Ed.), 'Handbook on Bipolar Membrane Technology' (Twente University Press, Enschede, Netherlands, 2000), Chapter 4.